The hemolymph of *Biomphalaria* snail vectors of schistosomiasis supports a diverse microbiome

Frédéric D. Chevalier*, Robbie Diaz, Marina McDew-White, Timothy JC. Anderson, Winka Le Clec'h*

Texas Biomedical Research Institute, PO Box 760549, San Antonio, TX 78258

Author information:

- Frédéric D. Chevalier*: fcheval@txbiomed.org – ORCID: 0000-0003-2611-8106
- Robbie Diaz: robbied@txbiomed.org
- Marina McDew-White: mwhite@txbiomed.org – ORCID: 0000-0001-7821-260X
- Timothy JC. Anderson: tanderso@txbiomed.org – ORCID: 0000-0002-0191-0204
- Winka Le Clec'h*: winkal@txbiomed.org – ORCID: 0000-0002-1111-2492

* Corresponding authors

Running title: The hemolymph microbiome of Biomphalaria snails

SUMMARY

The microbiome – the microorganism community that is found on or within an organism's body – is increasingly recognized to shape many aspects of its host biology and is a key determinant of health and disease. Microbiomes modulate the capacity of insect disease vectors (mosquitos, tsetse flies, sandflies) to transmit parasites and disease. We investigate the diversity and abundance of microorganisms within the hemolymph (*i.e.* blood) of *Biomphalaria* snails, the intermediate host for *Schistosoma mansoni*, using Illumina MiSeq sequencing of the bacterial 16S V4 rDNA. We sampled hemolymph from 5 snails from 6 different laboratory populations of *B. glabrata* and one population of *B. alexandrina*. We observed 279.84 ± 0.79 amplicon sequence variants (ASVs) per snail. There were significant differences in microbiome composition at the level of individual snails, snail populations and species. Snail microbiomes were dominated by Proteobacteria and Bacteroidetes while water microbiomes from snail tank were dominated by Actinobacteria. We investigated the absolute bacterial load using qPCR: hemolymph samples contained 2,784 ± 339 bacteria per µL. We speculate that the microbiome may represent a critical, but unexplored intermediary in the snail-schistosome interaction as hemolymph is in very close contact to the parasite at each step of its development.

32 **INTRODUCTION**

33 The microbiome – the community of microorganisms that inhabit both the human body and that of
34 multiple other phyla (Lee and Hase, 2014) – is increasingly recognized to play a critical role in many aspects of
35 biology and as a key determinant of health and disease. For example, the human gut microbiome is thought to
36 play a role in the development of diabetes, rheumatoid arthritis, muscular dystrophy, multiple sclerosis, and
37 obesity (Kinross *et al.*, 2011). In invertebrates, symbiotic bacteria are involved in synthesizing essential amino
38 acids or vitamins (Hosokawa *et al.*, 2010; Oliver *et al.*, 2010), in digesting cellulose (Brune, 2014), in protection
39 against parasites (Oliver *et al.*, 2010), in feminization and parthenogenesis (Werren *et al.*, 2008), and even in
40 speciation (Flintoft, 2013).

41 In host-parasite interactions, the host microbiome frequently plays an important role in the ability of
42 parasite to colonize its host. This tripartite interaction (i.e. host-microbiome-parasite/pathogen) has been
43 investigated widely in invertebrate hosts. Recent research on the widespread endosymbiotic bacteria *Wolbachia*
44 demonstrates that *Wolbachia*-infected mosquitoes are unable to transmit dengue fever (Slatko *et al.*, 2014).
45 This bacterium is now a major focus of efforts to control or eliminate dengue, and has stimulated new interest in
46 utilizing bacterial symbionts to modify disease vectors (Slatko *et al.*, 2014). Similarly, the aphid microbiome
47 protects these insects against parasitoid wasps (Oliver *et al.*, 2010), the microbiome of sandflies provides
48 protection against *Leishmania* infection (Sant'Anna *et al.*, 2014), while the microbiome of mosquitoes and tsetse
49 flies impedes infection by malaria parasites and trypanosomes respectively (Stathopoulos *et al.*, 2014).

50 Among human helminth parasites, schistosomes are the most important in terms of global morbidity
51 and mortality, infecting over 206 million people in 78 countries in 2016 (WHO), and causing more than 200,000
52 deaths per year. Schistosome parasites have a complex lifecycle, involving freshwater snails as intermediate
53 hosts and mammals as definitive hosts. In humans, adult schistosomes live in the blood vessels surrounding the
54 intestine, and pathology results from immune reactions to eggs which become trapped in the liver, resulting in
55 granulomas, calcification of blood vessels, portal hypertension and liver failure (van der Werf *et al.*, 2003; Colley

56 *et al.*, 2014). There is no licensed vaccine, and control is reliant on a single monotherapy (praziquantel) to which
57 resistance has been recorded, so there is an urgent need for alternative approaches to schistosome control.
58 Understanding the snail-schistosome interaction is therefore critical to develop these approaches. When a single
59 parasite larva (miracidium) penetrates a snail, this develops into a primary sporocyst, which then divides
60 asexually to generate multiple clonally-produced secondary sporocysts in the snail tissue. These produce
61 hundreds to tens of thousands of motile cercariae larvae that are released into the water where they penetrate
62 and infect the definitive host (human or rodent). Snail populations vary in susceptibility to schistosomes (Files
63 and Cram, 1949) and while genetics certainly plays a role (Tennessen *et al.*, 2015), the mechanisms determining
64 whether infections develop are poorly understood and the influence of the microbiome on schistosome parasite
65 development is currently unknown.

66 The *Biomphalaria* snail microbiome was firstly characterized using classical microbial culture methods
67 and biochemical characterization almost 40 years ago (Ducklow *et al.*, 1979). Bacteria were found in the whole
68 snail but also on its surface, gut and body cavity. With this relatively limited technique, the authors observed
69 changes in whole snail microbiome when those were moved between different environments (Ducklow *et al.*,
70 1979). More recently, two papers (Allan *et al.*, 2018; Huot *et al.*, 2020) have examined *Biomphalaria* spp.
71 microbiomes using deep sequencing of rDNA. Allan *et al.* (2018) showed that snails carrying alleles conferring
72 resistance to *Schistosoma mansoni* infection, show distinctive microbiomes from those carrying sensitive alleles,
73 suggesting possible links between the microbiome composition and *S. mansoni* susceptibility. Huot *et al.* (Huot
74 *et al.*, 2020) examined core microbiomes from several laboratory populations, showing a high specificity
75 between these microbiomes and their snail host populations, as well as complete congruence between core
76 microbiome and host phylogeny. Importantly, both these studies examined microbiomes of whole snails, so it is
77 unclear whether the bacteria characterized are from the gut, shell surface, mantle cavity or internal organs of
78 the snail, each of which may have a distinctive microbiome. Rather than characterize composite microbiomes
79 from whole snails, we focus on the microbiomes from a single tissue – the hemolymph (*i.e.*, invertebrate blood).

80 We chose this tissue because developing schistosome parasites are in continuous contact with the snail
81 hemolymph during the 30-day development within the snail. Therefore the hemolymph microbiome is likely to
82 be most relevant for understanding interactions between snails, bacteria and developing schistosomes.
83 Furthermore, evidence from other mollusk species provide a precedent for investigating the *Biomphalaria*
84 microbiome: hemolymphs from several fresh and seawater mollusks and crustaceans are known to harbor
85 specific microbiomes (Antunes *et al.*, 2010; Desriac *et al.*, 2014; Vezzulli *et al.*, 2018; Zhang *et al.*, 2018; Offret *et*
86 *al.*, 2019; Musella *et al.*, 2020; Table 1) that can be modified by environmental stress (Lokmer and Mathias
87 Wegner, 2015), pollutants (Leite *et al.*, 2017; Auguste *et al.*, 2019a) or pathogens (Vezzulli *et al.*, 2013; Lokmer
88 and Mathias Wegner, 2015).

89 In this study, we characterized the hemolymph microbiome of two *Biomphalaria spp.* freshwater snail
90 species (i.e. *B. glabrata* and *B. alexandrina*), both vectors of *S. mansoni* using a 16S rDNA approach. We
91 demonstrate that snail hemolymph harbors a diverse microbiome, and that different *Biomphalaria* species and
92 populations harbor distinctive hemolymph microbiomes that are independent of the water environment. As the
93 microbiome is critical in other host-parasite systems we speculate that it may represent a critical, but
94 unexplored, intermediary in the snail-schistosome interaction.

95

96 **RESULTS**

97 ***1) Library statistics***

98 We sequenced microbiomes from snail hemolymph and water samples from seven laboratory populations
99 (Table 2). For each population, we selected 5 snails, efficiently removed shell contaminants by cleaning the shell
100 surface with ethanol (Supp. Fig. 1) and collected hemolymph by heart puncture to avoid contamination from the
101 tegument. In parallel, we collected a sample of the tank water the snails were collected from. To test the
102 reproducibility of our protocol, we split each sample and prepared libraries independently for each half (Fig. 1).
103 After MiSeq sequencing, we obtained an average of 155,491.5 ± 29,277.9 reads per library (mean ± s.d.) (Supp.
104 Table 1). We retained on average 87 ± 0.04% of the initial reads after sequencing error filtering, 85 ± 0.03% of
105 the initial reads after denoising the data using the dada2 module, 73 ± 0.05% of the initial reads after merging
106 reads and 71 ± 0.06% of the initial reads after removing chimeras. Sequencing depth was relatively even
107 between sample types and replicates (Supp. Table 1). Rarefaction curve analysis of each library showed a
108 plateau, indicating that our sequencing effectively captured the microbiome diversity (Supp. Fig. 2). Taxonomy
109 assignment of the 16S rDNA sequences from all libraries revealed a total of 2,688 amplicon sequence variants
110 (ASVs). Among them, 897 had unassigned taxonomy as typically seen in microbiome study of non-model
111 organisms, with 39 (4.3%) being eukaryote contaminants (snails or others), 836 with match to uncultured
112 bacteria mainly, and 22 (2.5%) with no similarity to known sequences suggesting potential new bacterial or
113 archaeal species. The eukaryote contaminants and 5 ASVs with mitochondria or chloroplast assignment were
114 removed in subsequent analysis.

115

116 ***2) Microbiome diversity***

117 ***a) α diversity (microbial diversity within samples)***

118 We computed several α diversity indices (Table 3) to investigate the bacterial richness (the number of taxa) and
119 diversity (a composite measure of richness and abundance of bacterial taxa) within hemolymph and water
120 samples (Fig. 2). The observed species richness and the Chao1 index revealed that snail hemolymph had higher
121 bacterial richness than water, with the exception of the BgNMRI population. Overall, we found twice the
122 number of ASVs in snail hemolymph (279.84 ± 0.79; mean ± s.e.) than in the tank water (145.43 ± 4.02). Most of
123 the snail populations showed similar mean richness, with Bg26 showing the highest and BgNMRI the lowest. The
124 close similarity between the observed richness and the Chao1 index plots suggests that we effectively captured
125 rare taxa, consistent with the rarefaction analysis.

126 The bacterial richness of the hemolymph is correlated with a higher bacterial diversity as expected. The
127 Shannon diversity index showed lower mean diversity in the water when compared to the hemolymph. Among
128 the snail populations, we observed the highest mean diversity in Bg26 and Bg121 and the lowest in Bg36 and
129 BgNMRI. Individuals from the BgBS90 population showed the greatest variability between snails suggesting high
130 heterogeneity in this population. The Faith's phylogenetic diversity showed a similar trend: we observed a lower
131 diversity in the water while hemolymph displayed similar diversity across snail populations. This suggests that
132 the differences between snail populations observed with the Shannon index were likely due to differences in
133 evenness rather than in richness.

134 The Simpson indices for evenness and dominance were low for both hemolymph and water samples, in
135 accordance with the over representation of particular taxa. Hemolymph from Bg36 population, closely followed
136 by Ba population, showed the lowest evenness and the highest dominance of the snail populations. BgNMRI
137 snails, which had similar richness and diversity profile as Bg36 snails, showed slightly more evenness in their
138 bacterial community. Water samples, which consistently showed low richness and diversity, showed a
139 comparable evenness to snail samples but a higher dominance than some of the snail populations consistent
140 with the Shannon diversity index.

141 Data from the replicated libraries showed similar results. We obtained a strong correlation ($0.85 < R^2 <$
142 0.98, $p < 0.01$) between the replicated libraries (Supp. Fig. 3) when comparing the different indices, highlighting
143 the robustness and reproducibility of our protocol.

144

145 ***b) β diversity (microbial diversity between samples)***

146 We computed several β diversity indices to investigate how the bacterial communities discriminate between
147 each snail population (Fig. 3, Supp. Fig. 4). We first compared microbiomes using qualitative metrics that are
148 based on the presence or absence of bacterial taxa (Jaccard index) adjusted with phylogenetic distance
149 (unweighted unifrac index), independently of taxa abundance. We statistically compare these metrics using
150 Permanova analysis. These analyses demonstrate that water samples have significantly different bacterial
151 communities from the snail populations. Similarly, all pairwise comparisons between snail communities showed
152 statistically different composition. Comparisons of centroid distances revealed a significantly greater distance
153 between Ba and Bg than between each Bg populations in at least one of our replicate for both indices (Jaccard
154 index: Ba-Bg distance = 0.62, Bg populations distance = 0.57, $p = 0.021$; unweighted unifrac index: Ba-Bg
155 distance = 0.49, Bg populations distance = 0.45, $p = 0.010$). In addition, the principal component analysis from
156 the Jaccard index and, to a lesser extent, from the unweighted unifrac revealed clear groups: (i) Ba is distant
157 from all Bg snail populations as supported by centroid distances strongly suggesting that hemolymph
158 microbiome can discriminate snail species; (ii) Two clusters of Bg snails can be identified: the first cluster
159 comprises BgBS90, BgBRE, Bg121 and Bg36 (all from Brazil) and the second cluster comprises Bg26 and BgNMRI
160 (from Carribbean) (Fig. 3A-B).

161 We also compared populations of snails or water microbiome for the Jaccard and unweighted unifrac
162 indices using a β dispersion test (Fig. 3A-B). This test compares the homogeneity of β-diversity measures across
163 different sampling units (individual snails, or water from different tanks) between populations. All the snail

164 populations showed similar variance when compared to each other. In contrast, the water population showed
165 over dispersion when compared to all the snail populations. This may be explained by the fact that samples of
166 water come from different aquariums, each of them carrying characteristic bacteria, while individual snails
167 within a population come from the same tank.

168 We performed similar comparisons using quantitative metrics that take into account the abundance of
169 each bacterial taxa (Bray index) adjusted with phylogenetic information (weighted unifrac index). Comparisons
170 of Bray indices using a permanova analysis revealed that all snail populations and water showed different
171 composition from each other (Fig. 3C). We obtained similar results when adding phylogenetic information (Fig.
172 3D) except for the pairs Bg121-Bg36 and BgBS90-BgNMRI, suggesting that these microbiomes shared similar
173 abundant taxa between these pairs (Fig. 3D). Centroid distances were again a greater between Ba and Bg than
174 between each Bg populations in at least one of our replicate for both indices (Bray index: Ba-Bg distance = 0.69,
175 Bg populations distance = 0.63, $p = 0.014$; weighted unifrac index: Ba-Bg distance = 0.26, Bg populations distance
176 = 0.18, $p = 3.7 \times 10^{-5}$). These results suggest that abundant bacterial taxa drive the distinction between species
177 and within populations and revealed similar microbiomes in some genetically related snail populations (Bg121-
178 Bg36).

179

180 ***c) Taxonomic diversity***

181 We found dramatic differences between populations in terms of taxonomic composition of bacteria (Fig. 4).
182 While considering the populations, hemolymph microbiomes were dominated by bacteria from the phyla
183 Proteobacteria (in all Bg populations) and Bacteroidetes (in Ba population) while water microbiomes were
184 dominated by bacteria from the Actinobacteria phylum (Fig. 4C). These differences in dominating phyla reflect
185 the previous observations from the β diversity analyses: a clear distinction (i) between the water and snails and
186 (ii) between the two snail species (i.e., Bg and Ba). We also observed differences in proportion of bacteria from

187 minor phyla among the different snail populations. For instance, Bg26 showed a greater proportion of the
188 phylum Acidobacteria in most of the comparisons while BgNMRI and Ba showed the lowest proportion of the
189 phylum Verrucomicrobia in most of the comparisons (Supp. Table 2). These differences may reflect differences
190 in the physiology of these different populations. Microbiomes from snail samples (and at a lesser extent from
191 water samples) also contained a relatively high proportion of bacteria with unassigned taxa: 5% to 43% of ASVs
192 from snails while 0.2% to 17% of ASVs from the water were uncharacterized.

193 Individual snails from a population tended to show a similar taxonomic composition as they clustered
194 together (Fig. 4A). The relatedness between populations reflects what is observed with the qualitative analysis
195 of the β diversity (Fig. 3A-B).

196 We identified 93 snail and population specific ASVs not found in water and 1 water specific ASV not
197 found in snails (Supp. Fig. 5). The count of these ASVs ranged from 2 to 36,770 with a prevalence ranging from
198 1.19 to 73.81%. The Ba population showed most of the specific ASVs. Bg121, BgBRE, BgBS90 and BgNMRI
199 showed the lowest number of ASVs and Bg121, BgBRE, BgBS90 showed very low prevalence of these ASVs.
200 These snail specific ASVs suggest that they may be specifically adapted to their hosts.

201 We qualitatively compared our microbiome compositions to the main bacterial genus or family found in
202 other whole snail microbiome studies (Ducklow *et al.*, 1979, 1981; Allan *et al.*, 2018; Huot *et al.*, 2020). We
203 found bacteria from the *Pseudomonas*, *Acinetobacter*, *Aeromonas* genera and the Enterobacteriaceae family
204 identified in Caribbean field and laboratory populations (Ducklow *et al.*, 1979) in at least one individual of each
205 population, with the exception of *Acitenobacter,* which as absent from all BgNMRI snails. However, we did not
206 find bacteria from the *Vibrio*, *Pasteurella*, and *Moraxella* genera found in by Ducklow *et al.* (1979, 1981). We
207 also found bacteria from the *Gemmatimonas* genus in at least one individual snail from each population. This
208 genus was previously associated with BgBS90 snail genotypes showing resistance to schistosome infection (Allan
209 *et al.*, 2018). We did not find the *Micavibrio*, *Parabacteroides* and *Halobacteriovorax* genus identified by Allan *et*

210 *al*. (2018). We found bacteria from the *Pseudomonas*, *Pirellula*, *Candidatus*, *Mesorhizobium* genus and the
211 Flavobacteriaceae family previously identified in *Biomphalaria* snails (Huot *et al.*, 2020) but we did not find
212 bacteria from the *Mycoplasma*, *Planctomyces* and *Odyssella* genus found in the same study. These absence of
213 these bacterial taxa from our data set may reflect that these genera are in low concentration or truly absent
214 from the hemolymph, or that differences in the protocols (16S region amplified, primers, database, pipeline
215 used) may have precluded the identification from our current dataset.

216 Finally, the reproducibility of our protocol is again confirmed in this taxonomic analysis (Supp. Fig. 6). All
217 the replicated libraries clustered together, with the exception of one BgNMRI sample.

218

219 ***3) Microbiome density***

220 We investigated the bacterial density by performing real time quantitative PCR on our samples, and corrected
221 the results to estimate the number of bacteria (Fig. 5A-B). We quantified an average of 4,490 16S rDNA copies
222 per µL of sample (range: 186 to 59,487). We found the highest average copy number in BgNMRI and the lowest
223 in BgBRE and water (Fig. 5A) (Kruskal-Wallis test: X^2=26.494, df=7, p=0.0004108 followed by post-hoc pairwise
224 comparison test).

225 Bacteria usually carry more than one 16S gene copy in their genome (Větrovský and Baldrian, 2013). We
226 corrected the raw density data based on 16S copy number using the estimation of 16S copy number per ASV
227 computed by PiCRUST2. This normalization gave an average of 2,784 ± 339 (mean ± s.e.) (range: 186 to 17,578)
228 estimated bacteria per µL in snail samples and 1,475 ± 382 in water samples (range: 169 to 5,014) (Fig. 5B). This
229 did not change drastically the trend already observed with the raw copy number quantification. However,
230 normalization narrowed the global and per population variation and removed any significant differences
231 between populations (Kruskal-Wallis test: X^2=16.22, df=7, p=0.023). When considering an average volume of 100
232 µL of hemolymph per adult snail (personal observation) and an average of 2,784 estimated bacteria per µL in

233 snail individuals, the snail hemolymph should be inhabited by an average of 278,400 bacteria (range: 18,600 to
234 1,757,800).

235 We examined the correlation between the estimated bacteria density and the observed microbial
236 richness diversity. We found no correlation (Kendall's τ=-0.076, p-value=0.3). This confirms that we can safely
237 estimate microbial diversity without taking in account bacterial density.

238

239 ***4) Functional inference of the hemolymph microbiome***

240 The microbiome in hemolymph could have a functional role in the snail physiology, just as the gut microbiome
241 does in humans (Valdes *et al.*, 2018). We investigated the presence of particular metabolic pathways in snails
242 and water samples based on 16S taxonomy using the PiCRUST2 pipeline. We identified 36 and 4 pathways
243 overrepresented in hemolymph and water samples respectively, which is supported by our two technical
244 replicates (Supp. Table 3). The 36 overrepresented pathways in hemolymph were involved in synthesis of
245 vitamins/electron transporters, in degradation of sugar, amines and aromatic compounds, in nucleotide
246 metabolism and in fermentation.

247 The pathways overrepresented in water samples were involved in synthesis of molecules related to cell
248 wall, DNA synthesis, and detoxification. At least two out of the four overrepresented pathways are found in
249 bacteria from the Actinobacteria phylum, the dominant phylum found in water (Fig. 4).

250 In both snail and water samples, other differentially represented pathways were found in only one of
251 the two technical replicates. This could be due to differences in taxa representation and abundance and
252 highlight the sensitivity of metabolic inference to this factor.

253

254 **DISCUSSION**

255 ***1. Snail hemolymph supports a diverse microbiome.***

256 We have unambiguously shown the presence of diverse microbiomes in the snail hemolymph of one population
257 of *Biomphalaria alexandrina* and six populations of *B. glabrata.* The snail microbiome contains hemocytes that
258 protect against incoming microbes, so the existence of a flourishing microbiome in the hemolymph might seem
259 surprising to some. Three lines of argument suggest that the hemolymph microbiomes we have described are
260 real, rather than an artifact of our collection procedure:

261 i. The shell cleaning step of our protocol efficiently removed any traces of bacteria on the shell, ensuring
262 no contamination from the outside environment during the heart puncture (see Supp. Fig. 1 and section
263 1 of Experimental procedures).

264 ii. The bacterial diversity of the snail microbiomes is distinctive from that of the water in the tanks. The
265 hemolymph and water microbiome showed dramatic differences in dominating phyla (Proteobacteria
266 (for all the Bg populations), Bacteroidetes (for the Ba population), and Actinobacteria phylum in the
267 water microbiomes). The hemolymph microbiomes were more diverse than the water microbiomes
268 using multiple different diversity metrics. Finally, different species or populations of snails show
269 characteristic bacterial composition in their hemolymph. The hemolymph, and to a lesser extent, the
270 water samples harbor uncharacterized taxa: a third of the ASVs identified did not have a taxonomic
271 assignment.

272 iii. Bacteria were abundant in the hemolymph. We observed an average of 2,784 bacteria per microliter of
273 snail hemolymph, with a maximum of 17,578 in the BgNMRI population. Assuming 100µL hemolymph
274 per snail this equates to 278,400 bacteria, or 1,757,800 for BgNMRI.

275 Our demonstration that the *Biomphalaria* hemolymph contains a rich microbiome is consistent with published
276 reports detailing the microbiome from other mollusks, crustaceans (Braquart-Varnier *et al.*, 2008; Desriac *et al.*,

277 2014; Wang and Wang, 2015; Vezzulli *et al.*, 2018; Table 1) and also from insects (Blow and Douglas, 2019). The
278 intimate relationship between these organisms and their water environment and their semi-open vascular
279 system may prevent them from having a sterile hemolymph. Instead, they may use a tolerance strategy as
280 observed in the human gut (Swiatczak and Cohen, 2015). In insects, the presence of both transient and obligate
281 bacteria in the hemolymph is now recognized (Blow and Douglas, 2019) but only few bacterial taxa can survive
282 in such an environment. In contrast, our results show that the hemolymph of *Biomphalaria* snails is inhabited by
283 a highly diverse microbiome, suggesting that the snail hemolymph environment is more permissive.

284

285 ***2. Do genetics or the environment drive microbiome differences?***

286 Differences in microbial diversity between hemolymph samples reflected their species or populations of origin.
287 At the species level, *B. glabrata* and *B. alexandrina* always clustered apart based on both qualitative and
288 quantitative β diversity analysis. This was driven by the differences in bacterial taxa and their abundance
289 between the two species despite that all these snails were exposed to the same food and the same water source
290 at the time of the tank setup. Therefore, the differences in the microbial composition are likely to be genetically
291 controlled, reflecting the evolutionary distance between the two species. At the population level, we could
292 discriminate *B. glabrata* populations based on rare taxa (qualitative β diversity analysis). Interestingly, the
293 distance between population clusters was consistent with geographical origins: Brazilian populations (BgBRE,
294 BgBS90) clustered apart from the Caribbean population (BgNMRI), while inbred subpopulations from a cross
295 between snails of Caribbean and Brazilian origin (Bonner *et al.*, 2012) tended to cluster with the Caribbean
296 population (Bg26) or the Brazilian population (Bg36, Bg121). If genetics is the main driver, this would suggest
297 that microbiome selection at the population level is different from selection at the species level. However, a
298 strong influence of the environment could also explain this result: we sampled snails of each population from

299 single tanks. The rare taxa distinguishing microbiomes from different snail populations could also be a signature
300 of the tank microbiome.

301 An association between snail genetics and the composition of whole snail microbiome has been
302 observed previously (Allan *et al.*, 2018). In this particular case, specific genotypes at a locus involved in snail
303 compatibility with schistosome infection were linked to changes in two particular taxa (*Gemmatimonas*
304 *aurantiaca* and *Micavibrio aeruginosavorus*). This locus likely contains immune genes that could specifically
305 shape the whole snail microbiome. In addition, a recent analysis of whole snail microbiomes that included
306 several *Biomphalaria* species and *B. glabrata* populations is consistent with our observation regarding species
307 differentiation based on microbiome but failed to support *B. glabrata* population differentiation (Huot *et al.*,
308 2020). Three factors from the Huot *et al.* (Huot *et al.*, 2020) study could explain this difference: (i) the shell was
309 removed prior to DNA extraction: this may have resulted in significant loss of hemolymph, reducing the
310 contribution of hemolymph to the results, or (ii) their analysis focused on the core microbiome: excluding rare
311 taxa may have limited their ability to detect population differentiation, or (iii) the composite microbiome from
312 whole snails (including microbiomes from multiple different organs) was analyzed.

313 Previous studies on whole snail microbiomes using older, culture-based methodology showed a strong
314 influence of the environment: translocating *B. glabrata* from one river to another had a dramatic impact on
315 abundance of cultivable bacteria (Ducklow *et al.*, 1981). This change in microbiome could be due to uptake of
316 new bacteria from this new environment or could result from the stress of the translocation leading to the
317 modification of the immune system and consequently of the microbiome composition. To better understand the
318 relative role of genes and environment in controlling microbiome composition, classical genetic crosses, and
319 common garden rearing experiments will be needed.

320

321 ***3. Origin of the hemolymph microbiome***

322 Microorganisms can be acquired directly from the environment or transmitted vertically from the parents. We
323 observed shared bacterial taxa between snail hemolymph and water suggesting that exchanges between the
324 environment and the snail is likely to occur. Exchange could take place at two main sites: the mantle cavity and
325 the gut. The mantle cavity is likely involved in gas exchange between the hemolymph and the water (Jurberg *et*
326 *al.*, 1997). Pinocytosis at the mantle epithelium and loose vascular connective under it (Sullivan and Cheng,
327 1974) could promote active or passive acquisition of microorganisms. The microsporidium *Capsaspora*
328 *owczarzaki* was found in the mantle and pericardial explants strongly suggesting that microorganisms can pass
329 through the mantle cavity (Stibbs et al., 1979; Hertel et al., 2002). The gut and its surrounding hepatopancreas
330 where active phagocytosis happens (Van Weel, 1961) could be another site of microorganism acquisition.
331 Amoebae (Richards, 1968) and microsporidia (Richards and Sheffield, 1970) can infect the gut and
332 hepatopancreas suggesting that the complex gut microbiome (Van Horn et al., 2012) could colonize the
333 hemolymph through this route. This could be validated by comparing gut and hemolymph microbiome.

334 A second route of microbiome acquisition is a vertical transmission from parents to offspring.
335 Microorganisms could be selectively added to the egg yolk or the egg mass fluid (i.e. fluid surrounding the eggs
336 inside the egg mass) and could be integrated into the developing organism. Antimicrobial proteins have been
337 identified in both egg yolk (Baron *et al.*, 2013) and egg mass fluid (Hathaway *et al.*, 2010) which, in addition to
338 protecting the eggs from outside pathogens, could control the development of the transmitted microbiome.
339 Vertical transmission of microorganisms via the egg cytoplasm (Werren *et al.*, 2008) or after spreading them on
340 the egg surface (Abe *et al.*, 1995; Prado *et al.*, 2006) is common in invertebrates.

341

342 ***4. Microbiome functionality: transient passengers or co-evolved relationship***

343 The primary role of the hemolymph is to distribute nutrients to organs and defend the snail against infections.
344 The presence of a microbiome could result from a tolerance strategy to mitigate the high costs of maintaining a

345 sterile hemolymph and could be comprised of commensal microorganisms only. However, snails could have
346 evolved in order to take advantage of the presence of this microbiome. Hemolymph microbiomes could be
347 involved in providing nutrients to their snail host. Pathway inference analysis from our microbiome data showed
348 that hemolymph microbiome is enriched in pathways related to vitamin production. Vitamins are known to be
349 essential in egg production: snails raised in axenic conditions were not able to lay eggs except with a supplement
350 of vitamin E (Vieira, 1967). We did not find pathways involved in the production of this particular vitamin but for
351 others (B6, B12, K12) which may also have a role in snail physiology. The vitamins B6 (pyridoxine), B12
352 (cobalamin), and K12 (menaquinol) are essential to animals and could be released into the hemolymph by the
353 bacteria and absorbed by the snail tissues. We have also shown enrichment for other pathways like sugar and
354 polyamine metabolism which could serve only bacteria but could also be beneficial to snail hosts. Sugar
355 degradation is likely involved in energy generation for the bacteria. Polyamines are linked to bacterial growth
356 and survival by reducing oxidative stress (Murray Stewart *et al.*, 2018) which could be generated by the
357 presence of the hemocytes (Castillo *et al.*, 2020). Production of critical metabolites by the hemolymph
358 microbiome could support sustainable production of these metabolites. While pathway inference using 16S data
359 can give good indication of the pathways present and differentially represented between samples, a more
360 robust approach using metagenomics is required to confirm these inferences.

361 This microbiome could also be involved in snail defense either directly by controlling pathogens or
362 indirectly by stimulating the snail immune system or competing with pathogens. Snails are susceptible to
363 pathogens ranging from bacteria (Duval *et al.*, 2015) to multicellular parasites (Laidemitt *et al.*, 2017) such as
364 schistosomes causing damages to the snail organs.

365

366 ***5. Role of the hemolymph microbiome in the snail-schistosome interactions***

367 We hypothesize that hemolymph microbiome could be a third player in the interaction between the snail and its
368 schistosome parasite. Such tripartite interactions are increasingly recognized to modulate infection outcome
369 and could play a major role in evolution of host-parasite systems (Dheilly, 2014; Ford *et al.*, 2017). The
370 hemolymph is known to be involved in snail defense against schistosomes by the action of hemocytes and
371 humoral factors (Castillo *et al.*, 2020). Snail genetics has also been shown to be a major determinant of snail
372 resistance (Tennessen *et al.*, 2015). However, the microbiome could enhance or reduce snail resistance.
373 Enhancing resistance could occur by direct interaction with the parasite (through competition or parasite
374 infection) or by stimulation of the immune system. The microsporidia *C. owczarzaki* showed direct interaction
375 with *S. mansoni* sporocysts leading to their death while leaving the snail unharmed (Stibbs *et al.*, 1979; Hertel *et*
376 *al.*, 2002). These microsporidia were found in higher density in resistant snail populations (Stibbs *et al.*, 1979).
377 This could result from resistant snails actively selecting this particular microorganism. Furthermore, the
378 abundance of bacteria from the *Gemmatimonas* genus in whole snails has been associated with snail genotypes
379 linked to schistosome resistance (Allan *et al.*, 2018), genus which is also present in the hemolymph of our snail
380 populations. While it is unknown if the bacteria associated with the resistant genotype are actually involved in
381 resistance, this showed that genetic control of microbial composition occurs in snails and could influence
382 interactions between snails and schistosomes.

383 Beyond the snail hemolymph microbiome, we may also have to consider the influence of a potential
384 schistosome microbiome. Role of parasite microbiomes in host-parasite interactions is still poorly understood
385 but could be critical as stated by the Parasite Microbiome Project (Dheilly *et al.*, 2017). Non-human infecting
386 trematodes are known to harbor *Neorickettsia* endosymbionts (Jenkins *et al.*, 2019) and these might also be
387 present in schistosomes (Buddenborg *et al.*, 2017). In addition, schistosome larvae could acquire
388 microorganisms during their free living stages (miracidium and cercariae) or during their development into the
389 snail which could influence the outcome of the infection in snail and mammalian hosts. For instance, the
390 entomopathogenic nematodes *Heterorhabditis* and *Steinernema* rely on their gut bacteria to kill and consume

391 their insect host (Jenkins *et al.*, 2019). The schistosome microbiome, if present, could facilitate the development
392 of developing schistosome larvae inside the snail by disturbing the hemolymph microbiome or by interacting
393 with the snail immune system.

394 In addition to the fact that *Biomphalaria spp*. snails are intermediate hosts of *S. mansoni*, these snails
395 have several attractive features that make them a promising model system for studying invertebrate-
396 microbiome interactions. Namely (i) they are easy to grow in large numbers in aquaria or plastic trays and
397 experimentally tractable, (ii) they are relatively large and hemolymph can be easily sampled, (iii) as these snails
398 are hermaphrodite, inbred snail lines are easily generated by serial inbreeding to minimize host genetic effects
399 (Bonner *et al.*, 2012), (iv) improving genomic resources and tools for gene silencing are available (Knight *et al.*,
400 2011; Allan *et al.*, 2017). We anticipate that *Biomphalaria spp*. may join the list of non-traditional model
401 invertebrate species (Douglas, 2019) that are now being exploited for asking both pure and applied questions
402 about microbiome biology.

403

404 **EXPERIMENTAL PROCEDURES**

405 ***1)* Biomphalaria spp. *hemolymph collection***

406 *Biomphalaria spp.* freshwater snails are the intermediate host for schistosome trematode parasites. In this
407 study, we sampled only hemolymph (i.e. blood) from schistosome uninfected snails. All our *Biomphalaria spp*.
408 snails were reared in 10-gallon aquaria containing aerated freshwater at 26-28°C on a 12 hour light – 12 hour
409 dark photocycle and fed *ad libitum* on green leaf lettuce. An advantage of *Biomphalaria* snails is their large size
410 and their flat shell. This allows easy access to the heart and makes collection of ~80-100 µL of hemolymph
411 possible. All snails used in this study had a shell diameter between 10-15 mm.

412 For each individual snail, we disinfected the shell 3 times with 70% ethanol. We validated the effectiveness
413 of the disinfection method on an independent set of snails. We swabbed shells before and after the 70% ethanol
414 cleaning using sterile polyester tipped swabs (Puritan), extracted DNA and amplified 16S rDNA as described in
415 the next section. This showed no detectable rDNA and confirmed that collected hemolymph was not
416 contaminated with shell microbiome (Supp. Fig. 1). After shell cleaning, we collected the hemolymph by heart
417 puncture using a sterile 1 mL syringe and a sterile 22 gauge needle. The hemolymph collected was immediately
418 placed in a sterile 1.5 mL pre-cooled microtube on ice.

419 We collected hemolymph from 5 individual snails from each of 7 different populations of *Biomphalaria spp.*
420 (Table 2, Figure 1). We also sampled water from the aquaria where each *Biomphalaria spp*. populations were
421 raised as a control, to characterize the microbiome from the snails' environment. Immediately after collection,
422 samples were snap-frozen in liquid nitrogen and stored at -80˚C until processing. All the samples were collected
423 by a single experimenter, in a 2h window.

424

425 ***2) 16S rDNA library preparation and sequencing***

426 We extracted DNA from the snail hemolymph and water samples using the Blood and Tissue kit (Qiagen),
427 following the manufacturer's protocol, with minor modifications. All the DNA extractions were processed the
428 same day, using a single Blood and Tissue kit (Qiagen) kit, by a single experimenter. We also added blank
429 controls starting at the DNA extraction step to check for potential contaminant coming from the DNA extraction
430 kit and PCR reaction kit. To verify the reproducibility of our process for DNA extraction, library preparation and
431 sequencing, we split each hemolymph or water sample in two aliquots and processed them independently. For
432 each replicate sample, we extracted total DNA using 40 µL of the hemolymph or water samples. We incubated
433 each replicate for 45 minutes at 56˚C in a water bath. We recovered final gDNA in 50 µL of elution buffer
434 (Qiagen).

435 We prepared the 16S rDNA libraries under a biosafety cabinet to avoid contamination, and in triplicate to
436 avoid biases potentially introduced during PCR reaction step. We amplified 250 bp of the 16S rDNA V4 region
437 from bacteria and archaea, using specific primers (515f and 806rB) designed by the Earth Microbiome Project
438 (Apprill *et al.*, 2015). Each of the 515f forward primers were barcoded to allow sample identification. The 16S
439 rDNA V4 reaction mixture consisted of 4 µL of 1X 5 Prime Hot Master Mix (QuantaBio), 2 µL of sterile water, 1 µL
440 of 2 µM 515f barcoded primer, 1 µL of 2 µM 806rB primer (Supp. Table 4), and 2 µL of total gDNA template.
441 Libraries were amplified using the GeneAmp PCR system 9700 (Applied Biosystems) as follows: 95°C for 3
442 minutes, then 35 cycles of 95°C for 45 seconds, 50°C for 1 minute, 72°C for 90 seconds, then 72°C for 10
443 minutes. We electrophoresed 2 µL of each PCR product on agarose gel (2%) to check amplicon size, and absence
444 of contamination in the controls (Supp. File 7). We pooled the triplicate PCR products and the 24 µL of final
445 volume were purified by adding 44 µL of AMPure XP beads (Beckman Coulter), mixing with pipette followed by a
446 5 minute incubation. We separated the beads on a 96 well-plate magnetic device (5 minutes), discarded the
447 cleared solution from each well, and washed beads twice in 200 µL of freshly-prepared 70% ethanol (1 minute),
448 while maintaining the plate on the magnetic device. After drying beads (3 minutes), we eluted each library by
449 adding 20 µL of nuclease-free sterile water, mixing the beads and water by pipetting followed by a 2 minute

450 incubation. Then we separated the beads on the magnetic device (3 minutes) and placed the purified 16S rDNA
451 V4 barcoded libraries in a fresh 96 well-plate. All incubations were done at room temperature. We quantified
452 these libraries using the Picogreen quantification assay (Invitrogen) following the manufacturer's instructions.
453 Finally, we made an equimass pool of all the libraries using 15 ng of each library. We quantified the final pool
454 fragment size using the 4200 TapeStation (DNA screen tape, Agilent Technology) and molarity using the Kappa
455 library quantification kit for the Illumina sequencing platform (following the manufacturer's recommendations).
456 We sequenced the pool on an Illumina MiSeq sequencer at Texas Biomedical Research Institute (San Antonio,
457 Texas). Raw sequencing data are accessible from the NCBI Sequence Read Archive under BioProject accession
458 number PRJNA613098.

459

460 ***3) Sequence processing***

461 Commands and scripts used for the sequence processing and downstream analysis are available in a Jupyter
462 notebook on Zenodo (https://doi.org/10.5281/zenodo.4020011).

463 We demultiplexed the raw sequencing data obtained from the MiSeq using bcl2fastq (v2.17.1.14,
464 Illumina) with the default parameters. We used the fastq files generated as input for Qiime2 (v2019.4) (Bolyen
465 *et al.*, 2019). We checked the read quality from the results of the demux module. We then denoised and
466 clustered the sequences into amplicon sequence variants (ASVs) using the denoise-paired command from the
467 dada2 module with a max expected error of 5. We determined the taxonomy of the ASVs using the SILVA
468 database and the classify-consensus-vsearch command of the feature-classifier module using a 97% identity
469 threshold. ASVs with unassigned taxonomy were blasted against the NCBI nt database using megablast from
470 blast+ (v2.7.1) to identify eukaryotic contaminants for removal in downstream analysis. We used a relatively
471 lenient e-value threshold (1e-2) to increase our power of detection. To build a phylogenetic tree, we aligned the
472 ASVs and masked the highly variable positions using the mafft and mask commands from the alignment module.

473 Finally, we built and rooted a tree from the alignment using the fasttree and midpoint-root commands from the
474 phylogeny module.

475

476 ***4) Functional inference of the microbiome***

477 We inferred the microbiome's function using PiCRUST2 software (v2.1.4b). We used the Qiime2 processed data
478 and exported the ASV representative sequences of the taxonomy analysis and the abundance table. We placed
479 the sequences into the reference tree, performed hidden-state prediction of gene families and generated
480 metagenome prediction. We performed pathway-level inference and finally add functional description to the
481 generated files. Finally, we performed a differential pathway abundance using the ALDEx2 R package (v1.16.0)
482 (Fernandes *et al.*, 2014) on the unstratified pathway prediction.

483

484 ***5) Estimation of bacterial abundance by quantitative PCR***

485 We performed real time quantitative PCR (qPCR) reactions to estimate the number of bacterial 16S rDNA in each
486 hemolymph and water replicated sample. Reactions were performed in duplicate using the QuantStudio 5
487 (Applied Biosystems) as follows: 95°C for 10 minutes, then 40 cycles of 95°C for 15 seconds and 60°C for 1
488 minute. Duplicate reactions showing a difference in C_T greater than one were rerun. The reaction mixture
489 consisted of 5 µL of SYBR Green MasterMix (Applied Biosystems), 0.3 µL of 10 µM forward primer (515f without
490 barcode: GTGYCAGCMGCCGCGGTAA) and 10 µM reverse primer (806rB: GGACTACNVGGGTWTCTAAT)
491 amplifying 250 bp of the 16S rDNA V4 region, 3.4 µL of sterile water and 1 µL of total DNA template. We plotted
492 standard curves using seven dilutions of a purified 16S V4 rDNA amplicon (copies.μL^{-1}: 1.34×10^1, 1.34×10^2,
493 1.34×10^3, 1.34×10^4, 1.34×10^5, 1.34×10^6, 1.34×10^7). We produced the purified 16S V4 rDNA by amplification of
494 the V4 region of *Escherichia coli* XL 10-gold (Agilent) using TaKaRa Taq R001 AM kit (Clonetech) following the

495 manufacturer's protocol (PCR cycles: 95˚C for 10 min, [95˚C for 15 s, 50˚C for 30 s, 60˚C for 60 s] × 35 cycles,
496 60˚C for 10 min). We purified the PCR product using AMPure XP beads (Beckman Coulter) following the
497 manufacturer's protocol, and quantified it using Qubit dsDNA BR Assay kit (Invitrogen). We determined the
498 number of copies in the PCR product as follows: PCR product length × (average molecular mass of nucleotides
499 (330 $g.mol^{-1}$) × 2 strands) × Avogadro constant. The number of 16S V4 rDNA V4 copies in each sample was
500 estimated according to the standard curve (QuantStudio Design and Analysis Software). The primer pair
501 (515f/806rB) was chosen to allow direct comparison of qPCR values with Illumina MiSeq sequenced amplicons of
502 the same locus. We used the following equation to normalize the qPCR data:

$$q_{bacteria} = \left(q_{16S} \times \frac{50}{40}\right) \times \frac{1}{n_{ASV} \times n_{16S\ ASV}}$$

503 Where the the 16S copy number from the qPCR (q_{16S}) was first corrected with the dilution factor between
504 hemolymph and elution volume (40 and 50 µL, respectively) and this value was then normalized using the
505 estimated 16S copy per bacteria from PiCRUST2 ($n_{16S\ ASV}$) and the abundance of each bacteria from Qiime2 (n_{ASV})
506 (see previous section).

507

508 ***6) Statistical analysis***

509 All statistical analyzes and graphs were performed using R software (v3.5.1). We used several packages to
510 compute diversity statistics from the Qiime data: phyloseq (v1.26.1) (McMurdie and Holmes, 2013), microbiome
511 (v1.8.0), and picante (v1.8.1) (Kembel *et al.*, 2010). We compared α-diversity results using a pairwise Wilcoxon
512 test. We used the vegan (v2.5.4) and the pairwiseAdonis (v0.0.1) packages to perform β-dispersion and
513 Permanova tests, respectively. We used the DESeq2 package (v1.22.2) (Love *et al.*, 2014) to identify the
514 differentially represented phyla. We computed centroid distances from the different populations or species

515 using the usedist package (v0.4.0) and tested for significant differences using a t-test or a Wilcoxon test when
516 data did not follow a normal distribution (Shapiro test, $p < 0.05$).

517 We compared the microbial density between populations using a Kruskal-Wallis test (data not following
518 normal distribution; Shapiro test, $p < 0.05$) followed by pairwise comparison post-hoc test. We used Kendall's
519 tau coefficient to test the correlation between the estimated bacteria density and the observed microbial
520 richness. The confidence interval of significance was set to 95% and *p*-values less than 0.05 were considered as
521 significant.

522

523 **ACKNOWLEDGMENTS**

524 We thank Michael S. Blouin from Oregon State University for providing all the inbred *Biomphalaria glabrata*
525 snail lines (Bg26, Bg36 and Bg121) , Guillaume Mitta and Benjamin Gourbal (University of Perpignan, France) for
526 providing the BgBRE snails, Philip LoVerde (UT Health, San Antonio) and the Biomedical Research Institute
527 (NIAID Schistosomiasis Resource Center, Rockville, MD) for providing the BgNMRI and BgBS90 snails through
528 NIH-NIAID Contract HHSN272201700014I, and the Theodor Bilharz Research Institute (Giza, Egypt) for providing
529 *B. alexandrina* snails. We thank Shelley Cole and Vanessa Ayala (Texas Biomedical Research Institute) for help
530 with MiSeq sequencing. This research was supported by a Forum grant (14-04491 (FC, WL), a Cowles fellowship
531 (WL) from Texas Biomedical Research Institute and NIH grants (NIH R01AI133749 and R01AI123434 (TJCA)), and
532 was conducted in facilities constructed with support from Research Facilities Improvement Program grant C06
533 RR013556 from the National Center for Research Resources.

534

535 **CONFLICT OF INTEREST**

536 The authors declare no conflict of interest.

537

538

539 **REFERENCES**

540 Abe, Y., Mishiro, K., and Takanashi, M. (1995) Symbiont of brown-winged green bug, *Plautia stali* SCOTT.
541 *Japanese journal of applied entomology and zoology* **39**: 109–115.
542 Allan, E.R.O., Tennessen, J.A., Bollmann, S.R., Hanington, P.C., Bayne, C.J., and Blouin, M.S. (2017) Schistosome
543 infectivity in the snail, *Biomphalaria glabrata*, is partially dependent on the expression of Grctm6, a
544 Guadeloupe Resistance Complex protein. *PLoS neglected tropical diseases* **11**: e0005362.
545 Allan, E.R.O., Tennessen, J.A., Sharpton, T.J., and Blouin, M.S. (2018) Allelic variation in a single genomic region
546 alters the microbiome of the snail *Biomphalaria glabrata*. *The Journal of heredity* **109**: 604–609.
547 Antunes, F., Hinzmann, M., Lopes-Lima, M., Machado, J., and Martins da Costa, P. (2010) Association between
548 environmental microbiota and indigenous bacteria found in hemolymph, extrapallial fluid and mucus of
549 Anodonta cygnea (Linnaeus, 1758). *Microbial ecology* **60**: 304–309.
550 Apprill, A., McNally, S., Parsons, R., and Weber, L. (2015) Minor revision to V4 region SSU rRNA 806R gene
551 primer greatly increases detection of SAR11 bacterioplankton. *Aquat Microb Ecol* **75**: 129–137.
552 Auguste, M., Lasa, A., Pallavicini, A., Gualdi, S., Vezzulli, L., and Canesi, L. (2019a) Exposure to TiO_2 nanoparticles
553 induces shifts in the microbiota composition of *Mytilus galloprovincialis* hemolymph. *The Science of the*
554 *total environment* **670**: 129–137.
555 Auguste, M., Lasa, A., Pallavicini, A., Gualdi, S., Vezzulli, L., and Canesi, L. (2019b) Exposure to TiO_2 nanoparticles
556 induces shifts in the microbiota composition of *Mytilus galloprovincialis* hemolymph. *The Science of the*
557 *total environment* **670**: 129–137.
558 Baron, O.L., van West, P., Industri, B., Ponchet, M., Dubreuil, G., Gourbal, B., et al. (2013) Parental transfer of the
559 antimicrobial protein LBP/BPI protects *Biomphalaria glabrata* eggs against oomycete infections. *PLoS*
560 *pathogens* **9**: e1003792.
561 Blow, F. and Douglas, A.E. (2019) The hemolymph microbiome of insects. *Journal of insect physiology* **115**: 33–
562 39.
563 Bolyen, E., Rideout, J.R., Dillon, M.R., Bokulich, N.A., Abnet, C.C., Al-Ghalith, G.A., et al. (2019) Reproducible,
564 interactive, scalable and extensible microbiome data science using QIIME 2. *Nature biotechnology* **37**:
565 852–857.
566 Bonner, K.M., Bayne, C.J., Larson, M.K., and Blouin, M.S. (2012) Effects of Cu/Zn superoxide dismutase (sod1)
567 genotype and genetic background on growth, reproduction and defense in *Biomphalaria glabrata*. *PLoS*
568 *NeglTrop Dis* **6**: e1701.
569 Braquart-Varnier, C., Lachat, M., Herbinière, J., Johnson, M., Caubet, Y., Bouchon, D., and Sicard, M. (2008)
570 *Wolbachia* mediate variation of host immunocompetence. *PloS one* **3**: e3286.
571 Brune, A. (2014) Symbiotic digestion of lignocellulose in termite guts. *Nature reviews Microbiology* **12**: 168–180.
572 Buddenborg, S.K., Bu, L., Zhang, S.-M., Schilkey, F.D., Mkoji, G.M., and Loker, E.S. (2017) Transcriptomic
573 responses of Biomphalaria pfeifferi to Schistosoma mansoni: Investigation of a neglected African snail
574 that supports more S. mansoni transmission than any other snail species. *PLoS neglected tropical*
575 *diseases* **11**: e0005984.
576 Castillo, M.G., Humphries, J.E., Mourão, M.M., Marquez, J., Gonzalez, A., and Montelongo, C.E. (2020)
577 *Biomphalaria glabrata* immunity: Post-genome advances. *Developmental and comparative immunology*
578 **104**: 103557.
579 Colley, D.G., Bustinduy, A.L., Secor, W.E., and King, C.H. (2014) Human schistosomiasis. *Lancet* **383**: 2253–2264.
580 Desriac, F., Le Chevalier, P., Brillet, B., Leguerinel, I., Thuillier, B., Paillard, C., and Fleury, Y. (2014) Exploring the
581 hologenome concept in marine bivalvia: haemolymph microbiota as a pertinent source of probiotics for
582 aquaculture. *FEMS microbiology letters* **350**: 107–116.
583 Dheilly, N.M. (2014) Holobiont-Holobiont interactions: redefining host-parasite interactions. *PLoS pathogens* **10**:
584 e1004093.

585 Dheilly, N.M., Bolnick, D., Bordenstein, S., Brindley, P.J., Figuères, C., Holmes, E.C., et al. (2017) Parasite
586 microbiome project: Systematic investigation of microbiome dynamics within and across parasite-host
587 interactions. *mSystems* **2**:.
588 Douglas, A.E. (2019) Simple animal models for microbiome research. *Nature reviews Microbiology* **17**: 764–775.
589 Ducklow, H.W., Boyle, P.J., Maugel, P.W., Strong, C., and Mitchell, R. (1979) Bacterial flora of the schistosome
590 vector snail *Biomphalaria glabrata*. *Appl Environ Microbiol* **38**: 667–672.
591 Ducklow, H.W., Clausen, K., and Mitchell, R. (1981) Ecology of bacterial communities in the schistosomiasis
592 vector snail *Biomphalaria glabrata*. *Microb Ecol* **7**: 253–274.
593 Duval, D., Galinier, R., Mouahid, G., Toulza, E., Allienne, J.F., Portela, J., et al. (2015) A novel bacterial pathogen
594 of *Biomphalaria glabrata*: a potential weapon for schistosomiasis control? *PLoS neglected tropical*
595 *diseases* **9**: e0003489.
596 Fernandes, A.D., Reid, J.N., Macklaim, J.M., McMurrough, T.A., Edgell, D.R., and Gloor, G.B. (2014) Unifying the
597 analysis of high-throughput sequencing datasets: characterizing RNA-seq, 16S rRNA gene sequencing
598 and selective growth experiments by compositional data analysis. *Microbiome* **2**: 15.
599 Files, V.S. and Cram, E.B. (1949) A study on the comparative susceptibility of snail vectors to strains of
600 *Schistosoma mansoni*. *The Journal of Parasitology* **35**: 555–560.
601 Flintoft, L. (2013) Evolution: Speciation meets microbiomes. *Nature reviews Genetics* **14**: 598.
602 Ford, S.A., Williams, D., Paterson, S., and King, K.C. (2017) Co-evolutionary dynamics between a defensive
603 microbe and a pathogen driven by fluctuating selection. *Molecular ecology* **26**: 1778–1789.
604 Hathaway, J.J.M., Adema, C.M., Stout, B.A., Mobarak, C.D., and Loker, E.S. (2010) Identification of protein
605 components of egg masses indicates parental investment in immunoprotection of offspring by
606 *Biomphalaria glabrata* (gastropoda, mollusca). *Dev Comp Immunol* **34**: 425–435.
607 Hertel, L.A., Bayne, C.J., and Loker, E.S. (2002) The symbiont *Capsaspora owczarzaki*, nov. gen. nov. sp., isolated
608 from three strains of the pulmonate snail *Biomphalaria glabrata* is related to members of the
609 Mesomycetozoea. *Int J Parasitol* **32**: 1183–1191.
610 Hosokawa, T., Koga, R., Kikuchi, Y., Meng, X.-Y., and Fukatsu, T. (2010) Wolbachia as a bacteriocyte-associated
611 nutritional mutualist. *Proceedings of the National Academy of Sciences of the United States of America*
612 **107**: 769–774.
613 Huot, C., Clerissi, C., Gourbal, B., Galinier, R., Duval, D., and Toulza, E. (2020) Schistosomiasis vector snails and
614 their microbiota display a phylosymbiosis pattern. *Frontiers in microbiology* **10**: 3092.
615 Jenkins, T.P., Brindley, P.J., Gasser, R.B., and Cantacessi, C. (2019) Helminth microbiomes - a hidden treasure
616 trove? *Trends in parasitology* **35**: 13–22.
617 Jurberg, P., Cunha, R.A., and Rodrigues, M.L. (1997) Behavior of Biomphalaria glabrata Say, 1818 (Gastropoda:
618 Planorbidae) - 1. Morphophysiology of the mantle cavity. *Memorias do Instituto Oswaldo Cruz* **92**: 287–
619 295.
620 Kembel, S.W., Cowan, P.D., Helmus, M.R., Cornwell, W.K., Morlon, H., Ackerly, D.D., et al. (2010) Picante: R tools
621 for integrating phylogenies and ecology. *Bioinformatics (Oxford, England)* **26**: 1463–1464.
622 Kinross, J.M., Darzi, A.W., and Nicholson, J.K. (2011) Gut microbiome-host interactions in health and disease.
623 *Genome medicine* **3**: 14.
624 Knight, M., Miller, A., Liu, Y., Scaria, P., Woodle, M., and Ittiprasert, W. (2011) Polyethyleneimine (PEI) mediated
625 siRNA gene silencing in the *Schistosoma mansoni* snail host, *Biomphalaria glabrata*. *PLoS neglected*
626 *tropical diseases* **5**: e1212.
627 Laidemitt, M.R., Zawadzki, E.T., Brant, S.V., Mutuku, M.W., Mkoji, G.M., and Loker, E.S. (2017) Loads of
628 trematodes: discovering hidden diversity of paramphistomoids in Kenyan ruminants. *Parasitology* **144**:
629 131–147.
630 Lee, W.-J. and Hase, K. (2014) Gut microbiota-generated metabolites in animal health and disease. *Nature*
631 *chemical biology* **10**: 416–424.

632 Leite, L., Jude-Lemeilleur, F., Raymond, N., Henriques, I., Garabetian, F., and Alves, A. (2017) Phylogenetic
633 diversity and functional characterization of the Manila clam microbiota: a culture-based approach.
634 *Environmental science and pollution research international* **24**: 21721–21732.
635 Lewis, F.A., Stirewalt, M.A., Souza, C.P., and Gazzinelli, G. (1986) Large-scale laboratory maintenance of
636 *Schistosoma mansoni*, with observations on three schistosome/snail host combinations. *J Parasitol* **72**:
637 813–829.
638 Lokmer, A. and Mathias Wegner, K. (2015) Hemolymph microbiome of Pacific oysters in response to
639 temperature, temperature stress and infection. *The ISME journal* **9**: 670–682.
640 Love, M.I., Huber, W., and Anders, S. (2014) Moderated estimation of fold change and dispersion for RNA-seq
641 data with DESeq2. *Genome biology* **15**: 550.
642 McMurdie, P.J. and Holmes, S. (2013) phyloseq: an R package for reproducible interactive analysis and graphics
643 of microbiome census data. *PloS one* **8**: e61217.
644 Murray Stewart, T., Dunston, T.T., Woster, P.M., and Casero, R.A. (2018) Polyamine catabolism and oxidative
645 damage. *The Journal of biological chemistry* **293**: 18736–18745.
646 Musella, M., Wathsala, R., Tavella, T., Rampelli, S., Barone, M., Palladino, G., et al. (2020) Tissue-scale microbiota
647 of the Mediterranean mussel (Mytilus galloprovincialis) and its relationship with the environment. *The*
648 *Science of the total environment* **717**: 137209.
649 Offret, C., Jégou, C., Mounier, J., Fleury, Y., and Le Chevalier, P. (2019) New insights into the haemo- and coelo-
650 microbiota with antimicrobial activities from Echinodermata and Mollusca. *Journal of applied*
651 *microbiology* **126**: 1023–1031.
652 Oliver, K.M., Degnan, P.H., Burke, G.R., and Moran, N.A. (2010) Facultative symbionts in aphids and the
653 horizontal transfer of ecologically important traits. *Annual review of entomology* **55**: 247–266.
654 Ooi, M.C., Goulden, E.F., Smith, G.G., and Bridle, A.R. (2019) Haemolymph microbiome of the cultured spiny
655 lobster Panulirus ornatus at different temperatures. *Scientific reports* **9**: 1677.
656 Paraense, W.L. and Correa, L.R. (1963) Variation in susceptibility of populations of Australorbis glabratus to a
657 strain of Schistosoma mansoni. *Rev Inst Med Trop Sao Paulo* **5**: 15–22.
658 Pathirana, E., McPherson, A., Whittington, R., and Hick, P. (2019) The role of tissue type, sampling and nucleic
659 acid purification methodology on the inferred composition of Pacific oyster (Crassostrea gigas)
660 microbiome. *Journal of applied microbiology* **127**: 429–444.
661 Prado, S.S., Rubinoff, D., and Almeida, R.P.P. (2006) Vertical transmission of a pentatomid caeca-associated
662 symbiont. *Annals of the Entomological Society of America* **99**: 577–585.
663 Sant'Anna, M.R.V., Diaz-Albiter, H., Aguiar-Martins, K., Al Salem, W.S., Cavalcante, R.R., Dillon, V.M., et al. (2014)
664 Colonisation resistance in the sand fly gut: *Leishmania* protects *Lutzomyia longipalpis* from bacterial
665 infection. *Parasites & vectors* **7**: 329.
666 Slatko, B.E., Luck, A.N., Dobson, S.L., and Foster, J.M. (2014) *Wolbachia* endosymbionts and human disease
667 control. *Molecular and biochemical parasitology* **195**: 88–95.
668 Stathopoulos, S., Neafsey, D.E., Lawniczak, M.K.N., Muskavitch, M.A.T., and Christophides, G.K. (2014) Genetic
669 dissection of Anopheles gambiae gut epithelial responses to Serratia marcescens. *PLoS pathogens* **10**:
670 e1003897.
671 Stibbs, H.H., Owczarzak, A., Bayne, C.J., and DeWan, P. (1979) Schistosome sporocyst-killing amoebae isolated
672 from *Biomphalaria glabrata*. *Journal of invertebrate pathology* **33**: 159–170.
673 Sullivan, J.T. and Cheng, T.C. (1974) Structure and function of the mantle cavity of Biomphalaria glabrata
674 (Mollusca: Pulmonata). *Transactions of the American Microscopical Society* **93**: 416–420.
675 Swiatczak, B. and Cohen, I.R. (2015) Gut feelings of safety: tolerance to the microbiota mediated by innate
676 immune receptors. *Microbiology and immunology* **59**: 573–585.
677 Tennessen, J.A., Bonner, K.M., Bollmann, S.R., Johnstun, J.A., Yeh, J.-Y., Marine, M., et al. (2015) Genome-Wide
678 Scan and Test of Candidate Genes in the Snail Biomphalaria glabrata Reveal New Locus Influencing
679 Resistance to Schistosoma mansoni. *PLoS Negl Trop Dis* **9**: e0004077.

680 Theron, A., Rognon, A., Gourbal, B., and Mitta, G. (2014) Multi-parasite host susceptibility and multi-host
681 parasite infectivity: A new approach of the *Biomphalaria glabrata/Schistosoma mansoni* compatibility
682 polymorphism. *Infect Genet Evol* **26**: 80–88.
683 Valdes, A.M., Walter, J., Segal, E., and Spector, T.D. (2018) Role of the gut microbiota in nutrition and health.
684 *BMJ (Clinical research ed)* **361**: k2179.
685 Van Weel, P. (1961) The comparative physiology of digestion in molluscs. *American Zoologist* 245–252.
686 Větrovský, T. and Baldrian, P. (2013) The variability of the 16S rRNA gene in bacterial genomes and its
687 consequences for bacterial community analyses. *PloS one* **8**: e57923.
688 Vezzulli, L., Colwell, R.R., and Pruzzo, C. (2013) Ocean warming and spread of pathogenic vibrios in the aquatic
689 environment. *Microbial ecology* **65**: 817–825.
690 Vezzulli, L., Stagnaro, L., Grande, C., Tassistro, G., Canesi, L., and Pruzzo, C. (2018) Comparative 16SrDNA gene-
691 based microbiota profiles of the pacific oyster (*Crassostrea gigas*) and the mediterranean mussel
692 (*Mytilus galloprovincialis*) from a shellfish farm (ligurian sea, italy). *Microbial ecology* **75**: 495–504.
693 Vieira, E.C. (1967) Influence of vitamin E on reproduction of Biomphalaria glabrata under axenic conditions. *Am J*
694 *Trop Med Hyg* **16**: 792–796.
695 Wang, X.-W. and Wang, J.-X. (2015) Crustacean hemolymph microbiota: Endemic, tightly controlled, and
696 utilization expectable. *Molecular immunology* **68**: 404–411.
697 Wang, X.-W., Xu, J.-D., Zhao, X.-F., Vasta, G.R., and Wang, J.-X. (2014) A shrimp C-type lectin inhibits proliferation
698 of the hemolymph microbiota by maintaining the expression of antimicrobial peptides. *The Journal of*
699 *biological chemistry* **289**: 11779–11790.
700 van der Werf, M.J., de Vlas, S.J., Brooker, S., Looman, C.W.N., Nagelkerke, N.J.D., Habbema, J.D.F., and Engels, D.
701 (2003) Quantification of clinical morbidity associated with schistosome infection in sub-Saharan Africa.
702 *Acta Trop* **86**: 125–139.
703 Werren, J.H., Baldo, L., and Clark, M.E. (2008) Wolbachia: master manipulators of invertebrate biology. *Nature*
704 *reviews Microbiology* **6**: 741–751.
705 WHO World Health Organization. Schistosomiasis.
706 Zhang, Xinxu, Sun, Z., Zhang, Xusheng, Zhang, M., and Li, S. (2018) Hemolymph microbiomes of three aquatic
707 invertebrates as revealed by a new cell extraction method. *Applied and environmental microbiology* **84**:.
708

709 **TABLES**

710 **Table 1 – Aquatic organisms with known hemolymph microbiome.**

Organism (vernacular name) / phylum	Biotope	Hemolymph microbiome characterization	References
Crassostrea gigas (Pacific oyster) /Mollusk	Sea water	16S rRNA gene amplicon (V1-V2) pyrosequencing	Lokmer and Mathias Wegner, 2015
		16S rRNA gene amplicon HiSeq sequencing	Vezzulli *et al.*, 2018
		16S rRNA gene amplicon (V1-V3) sequencing	Pathirana *et al.*, 2019
		Bacterial culture / CFU* counting	Desriac *et al.*, 2014
Crassostrea angulate (Portuguese oyster) / Mollusk	Sea water	16S rRNA gene amplicon (V3-V4) HiSeq sequencing/bacterial culture	Zhang *et al.*, 2018[1]
Mytilus galloprovincialis (Mediterranean mussel) / Mollusk	Sea water	16S rRNA gene amplicon (V4) Ion Torrent sequencing	Auguste *et al.*, 2019b
		16S rRNA gene amplicon HiSeq sequencing	Musella *et al.*, 2020
Mytilus edulis *(Blue mussel)* / Mollusk	Sea water	Bacterial culture / CFU* counting	Desriac *et al.*, 2014
		16S rRNA gene amplicon sequencing	Offret *et al.*, 2019
Anodonta cygnea (Swan mussel) / Mollusk	Fresh water	Bacterial culture / CFU* counting	Antunes *et al.*, 2010
Pecten maximus (Great scallop) / Mollusk	Sea water	Bacterial culture / CFU* counting	Desriac *et al.*, 2014

Tapes rhomboides (Clam) / Mollusk	Sea water	Bacterial culture/ CFU* counting	Desriac *et al.*, 2014
Ruditapes philippinarum (Manila clam) / Mollusk	Sea water	Bacterial culture/16S rRNA gene amplicon sequencing	Leite *et al.*, 2017
Haliotis tuberculata (Abalone) /Mollusk	Sea water	16S rRNA gene amplicon sequencing	Offret *et al.*, 2019
Scylla paramamosain (Mud crab) / Arthropoda	Sea water	16S rRNA gene amplicon (V3-V4) HiSeq sequencing/bacterial culture	Zhang *et al.*, 2018[1]
Litopenaeus vannamei (Whiteleg shrimp) / Arthropoda	Sea water	16S rRNA gene amplicon (V3-V4) HiSeq sequencing/bacterial culture	Zhang *et al.*, 2018[1]
Marsupenaeus japonicas (Kuruma shrimp) / Arthropoda	Sea water	Bacterial culture/ CFU* counting	Wang *et al.*, 2014
Panulirus ornatus (Spiny lobster) / Arthropoda	Sea water	16S rRNA gene amplicon (V1-V3) pyrosequencing	Ooi *et al.*, 2019

711 [1]For additional references on hemolymph microbiome related studies, see **Table 1** from Zhang *et al.*, 2018.

712 *CFU: Colony Forming Unit

713

714

715

716

717

718

719 **Table 2 – Snail laboratory populations used in this study and their characteristics.**

***Biomphalaria* species**	***Biomphalaria laboratory* population**	**Origin (Country, town, snail cross)**	**Albinism**	**Inbreeding**	**References**
B. alexandrina	Ba	Egypt	No	No	Theodor Bilharz Research Institute, Egypt
B. glabrata	BgBS90	Brazil	No	No	Paraense and Correa, 1963
	BgBRE	Brazil (Recife)	Yes	No	Theron *et al.*, 2014
	BgNMRI	Puerto Rico	Yes	No	Lewis *et al.*, 1986
	Bg26	BgM line derived (cross between a Brazilian and a Puerto Rican snail)	Yes	Yes	Bonner *et al.*, 2012
	Bg36		Yes	Yes	
	Bg121		Yes	Yes	

720

721

722 **Table 3 – Description of α diversity indices used.**

Index	Description
Observed richness	Raw number of ASVs
Chao1 richness	Estimation of the true richness by adjusting the raw number of ASVs for rare taxa
Faith's Phylogenetic diversity index	Richness index based on phylogenetic distance between ASVs
Shannon index	Measure of heterogeneity in taxa representation (evenness × richness)
Simpson evenness index	Measure of true evenness of taxa within a sample independently of taxa richness. A value close to 0 means that the taxa are unevenly distributed in a sample.
Simpson dominance index	Measure of taxa diversity within a sample. This index is weighted towards the most abundant taxa and influenced by taxa richness. A value close to 0 means that the sample is dominated by few taxa.

723

724

725 **FIGURES**

726 **Fig. 1 – Site of hemolymph sampling and workflow of the library preparation and the analysis. A.** Snail
727 hemolymph was sampled directly by heart puncture using a syringe. Left panel shows the position of the heart
728 (arrow) on an albino snail. Right panel shows a schematic representation of the puncture. **B.** Work flow of the
729 sample preparation and data processing.

730 **Fig. 2 – α diversity indices.** Six different alpha diversity indices were computed (see Table 2 for index
731 description) revealing that snail hemolymph harbors bacteria communities and those communities are richer
732 and more diverse that those of the water. Variation in diversity exists between snail populations. All these
733 bacterial communities are dominated by characteristic bacterial species. Each box plot represents the median
734 and the interquartile ranges of the distribution. Groups (i.e. snail populations or tank water) not connected by
735 the same letter are significantly different (post-hoc test).

736 **Fig. 3 – β diversity indices**. For each index (A. Jaccard, B. Unweighted unifrac, C. Bray, D. Weighted unifrac), the
737 first two axes of the principal coordinates analysis (PCoA) are represented. The two first indices represent a
738 qualitative measure (absence or presence of bacterial taxa) while the two last are quantitative (adjusted with
739 taxa abundance). The matrices on the right side of each index showed the significance level of the Permanova
740 test (differences between populations) and the β dispersion test (homogeneity of variance between
741 populations). All four indices showed that water microbiome was different from snail hemolymph microbiomes,
742 that the two species of snail (*B. glabrata* and *B. alexandrina*) can be differentiated on a quantitative and
743 qualitative approaches, and that *B. glabrata* populations were differentiated based on rare taxa (qualitative
744 aspect) and this differentiation could be linked to their geographic origin. The ellipse represents the multivariate
745 normal distribution.

746 **Fig. 4 – Taxonomic diversity in each sample and populations**. **A.** Dendrogram representing the distance
747 between samples based on their microbiome composition. Number under each node represents bootstrap

748 values from 1,000 iterations. Samples from the same population cluster together and links between populations
749 reflects results obtained from the beta-diversity analysis. **B and C**. Relative abundance of the different phyla
750 present in each samples from the dendrogram (B) and in each corresponding populations (C). Water microbiome
751 showed dramatic differences when compared to snail hemolymph microbiomes. Snail microbiomes showed also
752 specificities between populations.

753 **Fig. 5 – Comparison of microbial density and diversity**. **A.** Raw 16S copy number per microliter of hemolymph
754 and water sample quantified using qPCR. **B.** Estimation of bacteria per microliter after adjusting 16S copy
755 number using PiCRUST2 input. **C.** Correlation between observed number of ASVs and estimated bacteria
756 number. The number of bacteria present in a sample does not correlate with the number of ASVs observed. The
757 dot colors are consistent with the population colors in the above panels. The different letters on panel A and B
758 indicate significant differences in density means. Groups (i.e. snail populations or tank water) not connected by
759 the same letter are significantly different (pairwise comparison post-hoc test, $p < 0.05$).

760

761 **SUPPLEMENTARY MATERIALS**

762 **Supp. Fig. 1 – Shell cleaning effectiveness.** We swabbed snail shells before and after ethanol cleaning and
763 amplified 16S rDNA to test the effectiveness of the cleaning methods. This was done on a snail of each
764 population. L corresponds to the 100 bp ladder; 1 and 2 correspond to swab samples before and after 70%
765 ethanol shell cleaning, respectively; + and - correspond to positive (*E. coli* DNA) and negative (water only) PCR
766 controls.

767 **Supp. Fig. 2 – Library rarefaction curve for each snail population.** Curves represent the number of bacterial
768 species identified while subsampling a defined number of 16S V4 sequences. Each curve reached a plateau
769 phase indicating that sampling more sequences did not reveal new bacterial species and therefore that the
770 sequencing was sufficient to capture all the diversity present in the hemolymph sample.

771 **Supp. Fig. 3 – Correlation of α diversity indices between replicates.** For the six different alpha diversity indices,
772 we performed a correlation analysis between the two replicates and showed that they are highly correlated
773 confirming the reproducibility of our methods. *R* refers to the Pearson's correlation coefficient (ranging from 0
774 for no correlation, to 1 for perfect correlation) and *p* refers to the p-value associated.

775 **Supp. Fig. 4 – Principal coordinates analysis (PCoA) of β diversity indices.** For each index (Jaccard, Unweighted
776 unifrac, Bray, Weighted unifrac), the first three axes of the PCoA are represented in pairwise. The two first
777 indices represent a qualitative measure (absence or presence of bacterial taxa) while the two last are
778 quantitative (adjusted with taxa abundance). A and B refer to replicate 1 and 2, respectively.

779 **Supp. Fig. 5 – Heatmap of the 94 specific ASVs to snail hemolymph or water microbiomes.** ASVs found in either
780 snails but not water, or in water only, on in specific population of snails.

781 **Supp. Fig. 6 – Taxonomic diversity in each replicated sample.** This figure is similar to Fig. 4 with the addition of
782 the replicated libraries. Each replicated library clustered together showing the reproducibility of the protocol.

783 **Supp. Fig. 7 - 16S library preparation gels.** Each library was prepared in triplicate in separated plates. Failed
784 amplifications were run again (plate 4). Gels showed absence of amplification in the negative control (sterile
785 water treated alongside samples).

786

787 **Supp. Table 1 – Library statistics.**

788 **Supp. Table 2 – Differentially represented phyla.**

789 **Supp. Table 3 – Differentially represented metabolic pathways in snails and water samples.**

790 **Supp. Table 4 – Earth Microbiome Project primers used for generating each library.**

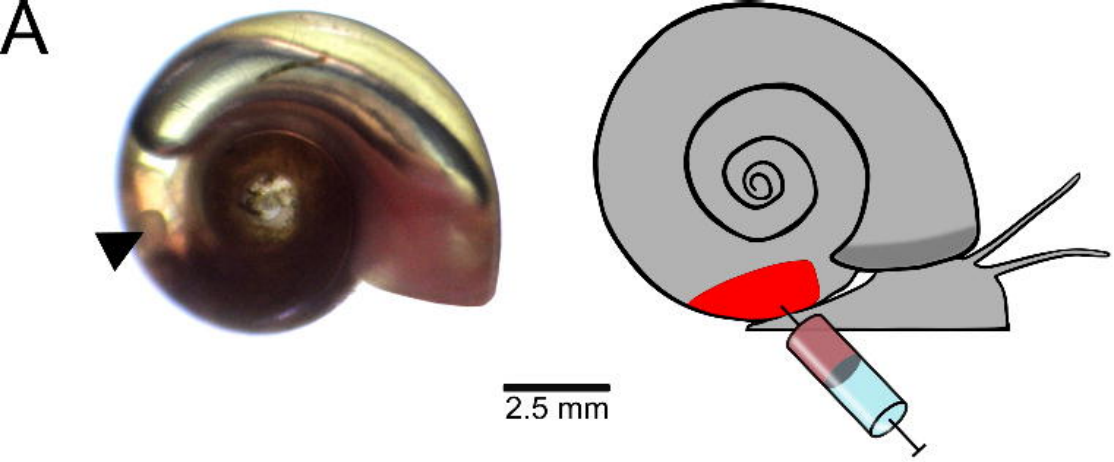
A
2.5 mm

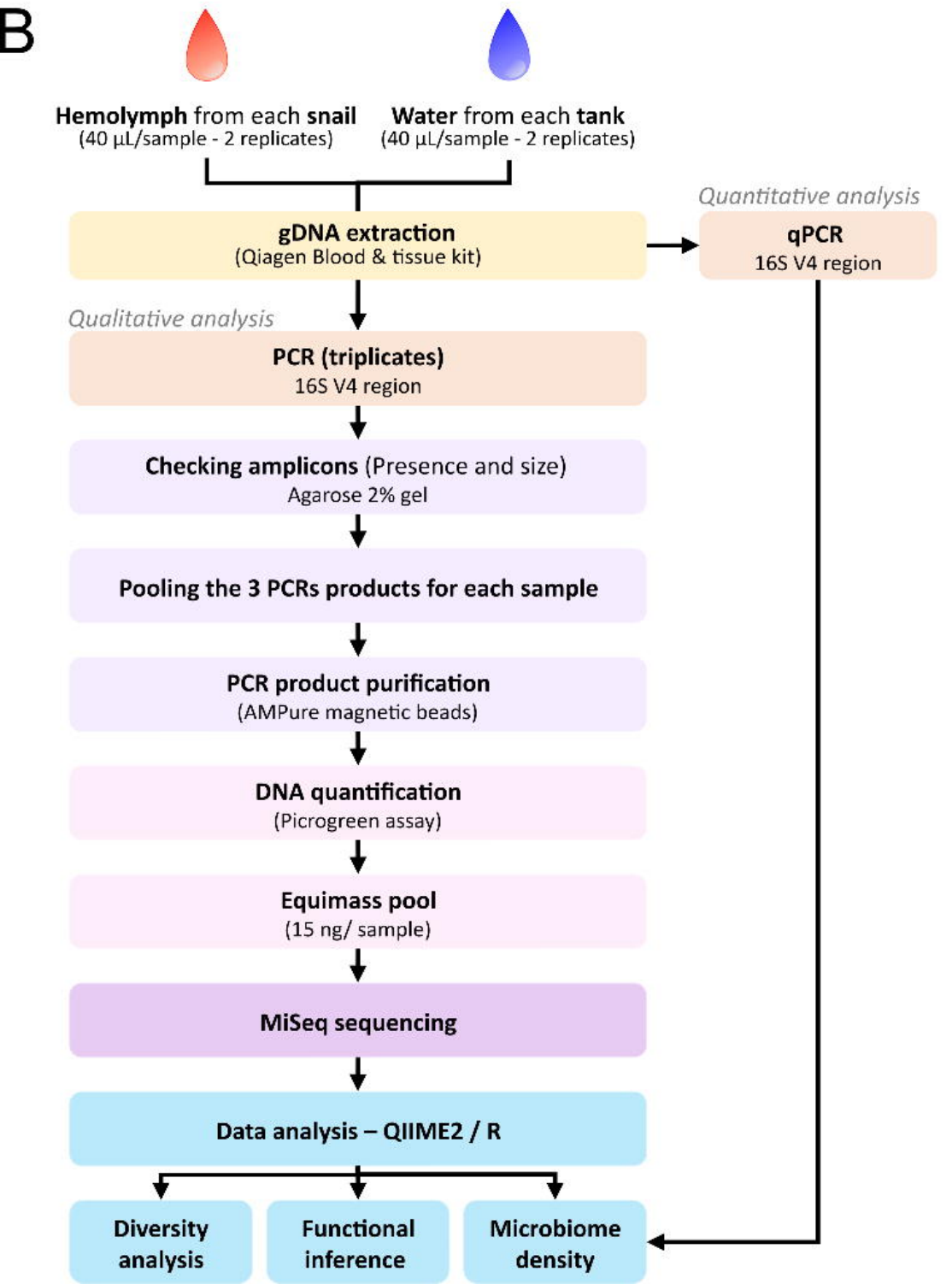
B
Hemolymph from each snail
(40 µL/sample - 2 replicates)
Water from each tank
(40 µL/sample - 2 replicates)
gDNA extraction
(Qiagen Blood & tissue kit)
Quantitative analysis
qPCR
16S V4 region
Qualitative analysis
PCR (triplicates)
16S V4 region
Checking amplicons (Presence and size)
Agarose 2% gel
Pooling the 3 PCRs products for each sample
PCR product purification
(AMPure magnetic beads)
DNA quantification
(Picrogreen assay)
Equimass pool
(15 ng/ sample)
MiSeq sequencing
Data analysis – QIIME2 / R
Diversity analysis
Functional inference
Microbiome density

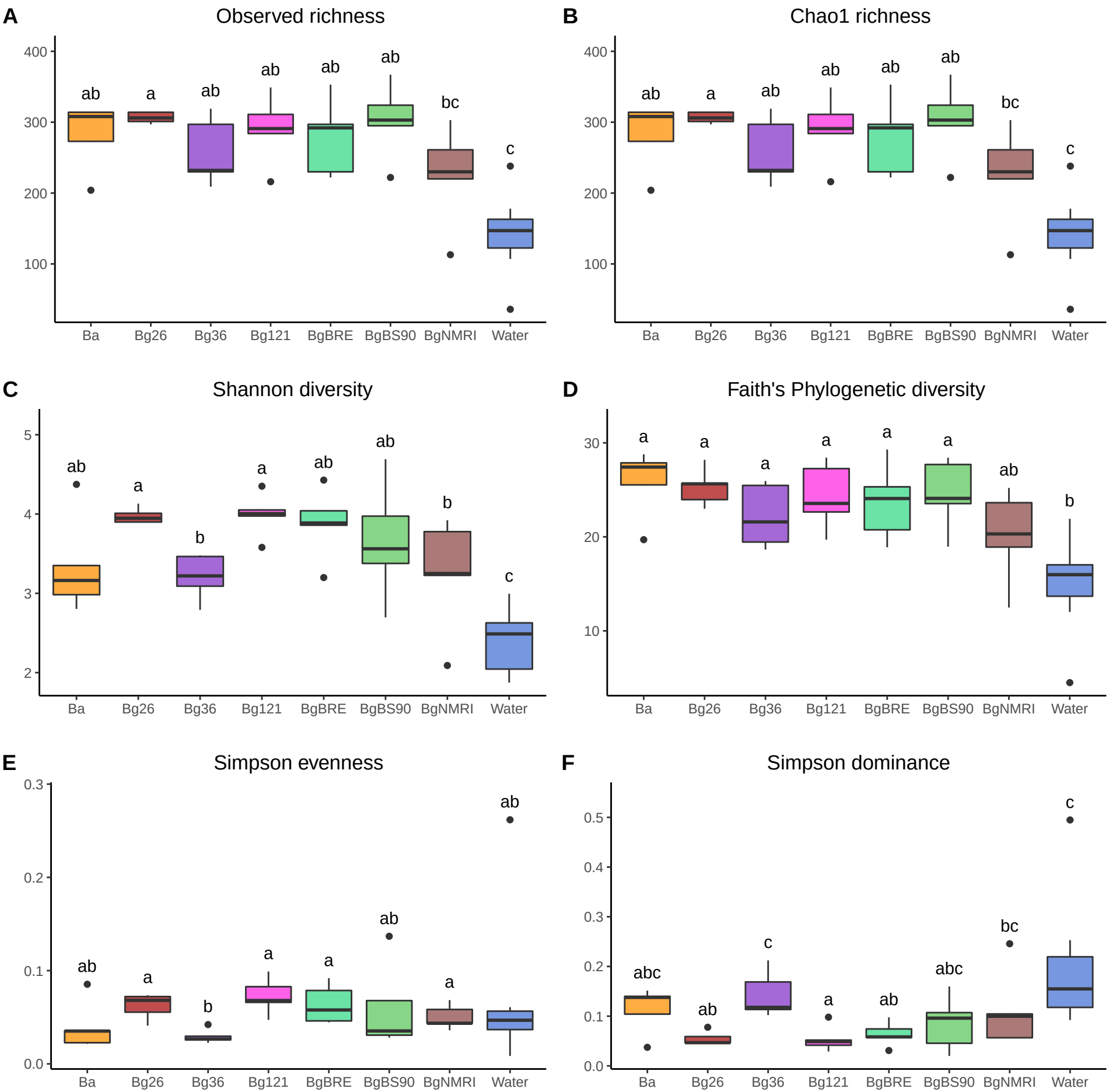
A
Observed richness
400
300
200
100
ab
a
ab
ab
ab
ab
bc
c
Ba
Bg26
Bg36
Bg121
BgBRE
BgBS90
BgNMRI
Water
B
Chao1 richness
400
300
200
100
ab
a
ab
ab
ab
ab
bc
c
Ba
Bg26
Bg36
Bg121
BgBRE
BgBS90
BgNMRI
Water
C
Shannon diversity
5
4
3
2
ab
a
b
a
ab
ab
b
c
Ba
Bg26
Bg36
Bg121
BgBRE
BgBS90
BgNMRI
Water
D
Faith's Phylogenetic diversity
30
20
10
a
a
a
a
a
a
ab
b
Ba
Bg26
Bg36
Bg121
BgBRE
BgBS90
BgNMRI
Water
E
Simpson evenness
0.3
0.2
0.1
0.0
ab
a
b
a
a
ab
a
ab
Ba
Bg26
Bg36
Bg121
BgBRE
BgBS90
BgNMRI
Water
F
Simpson dominance
0.5
0.4
0.3
0.2
0.1
0.0
abc
ab
c
a
ab
abc
bc
c
Ba
Bg26
Bg36
Bg121
BgBRE
BgBS90
BgNMRI
Water

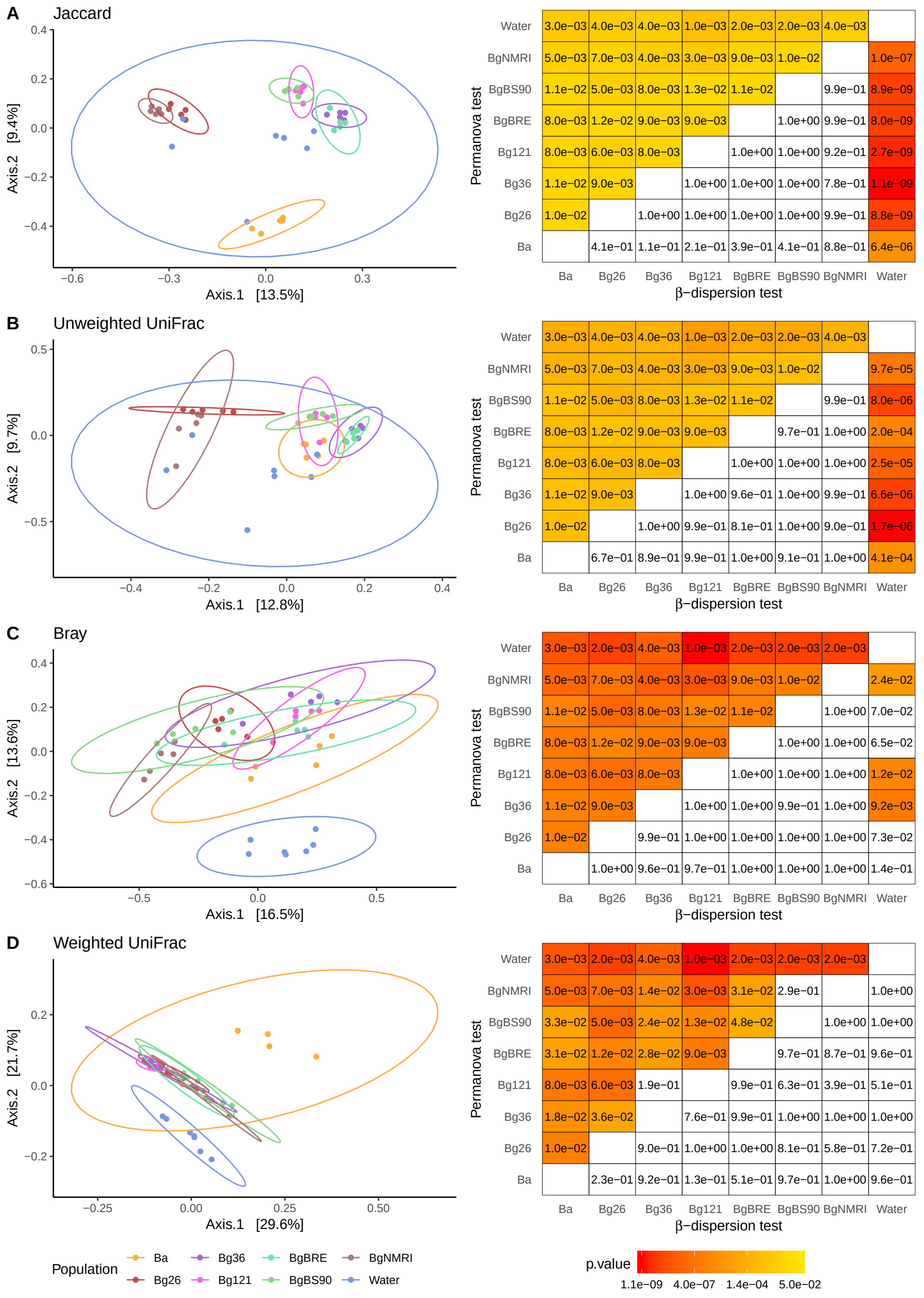
A
Jaccard
Axis.2 [9.4%]
Axis.1 [13.5%]
Permanova test
β−dispersion test
Water 3.0e−03 4.0e−03 4.0e−03 1.0e−03 2.0e−03 2.0e−03 4.0e−03
BgNMRI 5.0e−03 7.0e−03 4.0e−03 3.0e−03 9.0e−03 1.0e−02 1.0e−07
BgBS90 1.1e−02 5.0e−03 8.0e−03 1.3e−02 1.1e−02 9.9e−01 8.9e−09
BgBRE 8.0e−03 1.2e−02 9.0e−03 9.0e−03 1.0e+00 9.9e−01 8.0e−09
Bg121 8.0e−03 6.0e−03 8.0e−03 1.0e+00 1.0e+00 9.2e−01 2.7e−09
Bg36 1.1e−02 9.0e−03 1.0e+00 1.0e+00 1.0e+00 7.8e−01 1.1e−09
Bg26 1.0e−02 1.0e+00 1.0e+00 1.0e+00 1.0e+00 9.9e−01 8.8e−09
Ba 4.1e−01 1.1e−01 2.1e−01 3.9e−01 4.1e−01 8.8e−01 6.4e−06
Ba Bg26 Bg36 Bg121 BgBRE BgBS90 BgNMRI Water
B
Unweighted UniFrac
Axis.2 [9.7%]
Axis.1 [12.8%]
Permanova test
β−dispersion test
Water 3.0e−03 4.0e−03 4.0e−03 1.0e−03 2.0e−03 2.0e−03 4.0e−03
BgNMRI 5.0e−03 7.0e−03 4.0e−03 3.0e−03 9.0e−03 1.0e−02 9.7e−05
BgBS90 1.1e−02 5.0e−03 8.0e−03 1.3e−02 1.1e−02 9.9e−01 8.0e−06
BgBRE 8.0e−03 1.2e−02 9.0e−03 9.0e−03 9.7e−01 1.0e+00 2.0e−04
Bg121 8.0e−03 6.0e−03 8.0e−03 1.0e+00 1.0e+00 1.0e+00 2.5e−05
Bg36 1.1e−02 9.0e−03 1.0e+00 9.6e−01 1.0e+00 9.9e−01 6.6e−06
Bg26 1.0e−02 1.0e+00 9.9e−01 8.1e−01 1.0e+00 9.0e−01 1.7e−06
Ba 6.7e−01 8.9e−01 9.9e−01 1.0e+00 9.1e−01 1.0e+00 4.1e−04
Ba Bg26 Bg36 Bg121 BgBRE BgBS90 BgNMRI Water
C
Bray
Axis.2 [13.6%]
Axis.1 [16.5%]
Permanova test
β−dispersion test
Water 3.0e−03 2.0e−03 4.0e−03 1.0e−03 2.0e−03 2.0e−03 2.0e−03
BgNMRI 5.0e−03 7.0e−03 4.0e−03 3.0e−03 9.0e−03 1.0e−02 2.4e−02
BgBS90 1.1e−02 5.0e−03 8.0e−03 1.3e−02 1.1e−02 1.0e+00 7.0e−02
BgBRE 8.0e−03 1.2e−02 9.0e−03 9.0e−03 1.0e+00 1.0e+00 6.5e−02
Bg121 8.0e−03 6.0e−03 8.0e−03 1.0e+00 1.0e+00 1.0e+00 1.2e−02
Bg36 1.1e−02 9.0e−03 1.0e+00 1.0e+00 9.9e−01 1.0e+00 9.2e−03
Bg26 1.0e−02 9.9e−01 1.0e+00 1.0e+00 1.0e+00 1.0e+00 7.3e−02
Ba 1.0e+00 9.6e−01 9.7e−01 1.0e+00 1.0e+00 1.0e+00 1.4e−01
Ba Bg26 Bg36 Bg121 BgBRE BgBS90 BgNMRI Water
D
Weighted UniFrac
Axis.2 [21.7%]
Axis.1 [29.6%]
Permanova test
β−dispersion test
Water 3.0e−03 2.0e−03 4.0e−03 1.0e−03 2.0e−03 2.0e−03 2.0e−03
BgNMRI 5.0e−03 7.0e−03 1.4e−02 3.0e−03 3.1e−02 2.9e−01 1.0e+00
BgBS90 3.3e−02 5.0e−03 2.4e−02 1.3e−02 4.8e−02 1.0e+00 1.0e+00
BgBRE 3.1e−02 1.2e−02 2.8e−02 9.0e−03 9.7e−01 8.7e−01 9.6e−01
Bg121 8.0e−03 6.0e−03 1.9e−01 9.9e−01 6.3e−01 3.9e−01 5.1e−01
Bg36 1.8e−02 3.6e−02 7.6e−01 9.9e−01 1.0e+00 1.0e+00 1.0e+00
Bg26 1.0e−02 9.0e−01 1.0e+00 1.0e+00 8.1e−01 5.8e−01 7.2e−01
Ba 2.3e−01 9.2e−01 1.3e−01 5.1e−01 9.7e−01 1.0e+00 9.6e−01
Ba Bg26 Bg36 Bg121 BgBRE BgBS90 BgNMRI Water
Population
Ba Bg36 BgBRE BgNMRI
Bg26 Bg121 BgBS90 Water
p.value
1.1e−09 4.0e−07 1.4e−04 5.0e−02

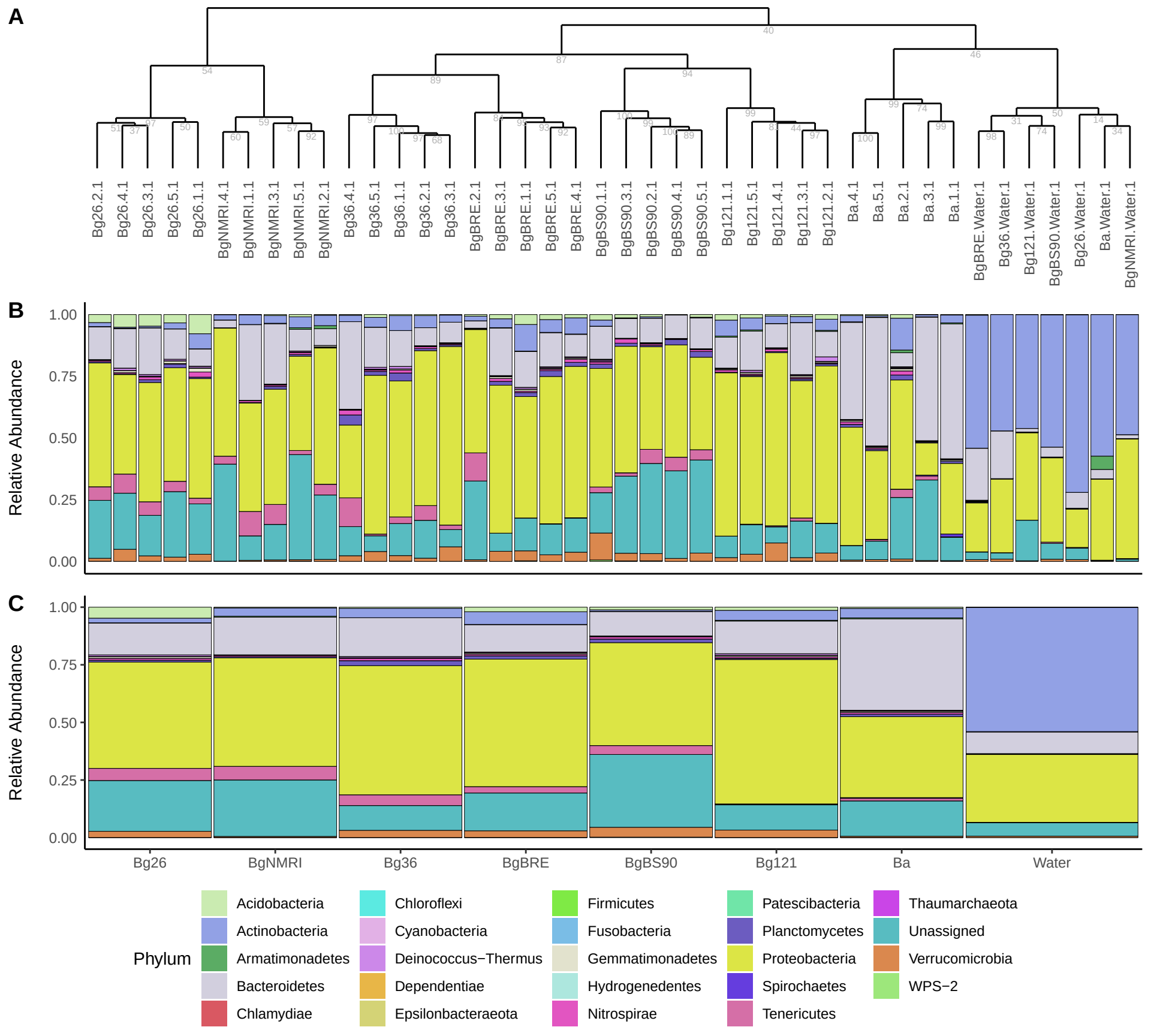
A
B
C
Relative Abundance
1.00
0.75
0.50
0.25
0.00
Bg26.2.1
Bg26.4.1
Bg26.3.1
Bg26.5.1
Bg26.1.1
BgNMRI.4.1
BgNMRI.1.1
BgNMRI.3.1
BgNMRI.5.1
BgNMRI.2.1
Bg36.4.1
Bg36.5.1
Bg36.1.1
Bg36.2.1
Bg36.3.1
BgBRE.2.1
BgBRE.3.1
BgBRE.1.1
BgBRE.5.1
BgBRE.4.1
BgBS90.1.1
BgBS90.3.1
BgBS90.2.1
BgBS90.4.1
BgBS90.5.1
Bg121.1.1
Bg121.5.1
Bg121.4.1
Bg121.3.1
Bg121.2.1
Ba.4.1
Ba.5.1
Ba.2.1
Ba.3.1
Ba.1.1
BgBRE.Water.1
Bg36.Water.1
Bg121.Water.1
BgBS90.Water.1
Bg26.Water.1
Ba.Water.1
BgNMRI.Water.1
Bg26
BgNMRI
Bg36
BgBRE
BgBS90
Bg121
Ba
Water
Phylum
Acidobacteria
Actinobacteria
Armatimonadetes
Bacteroidetes
Chlamydiae
Chloroflexi
Cyanobacteria
Deinococcus−Thermus
Dependentiae
Epsilonbacteraeota
Firmicutes
Fusobacteria
Gemmatimonadetes
Hydrogenedentes
Nitrospirae
Patescibacteria
Planctomycetes
Proteobacteria
Spirochaetes
Tenericutes
Thaumarchaeota
Unassigned
Verrucomicrobia
WPS−2

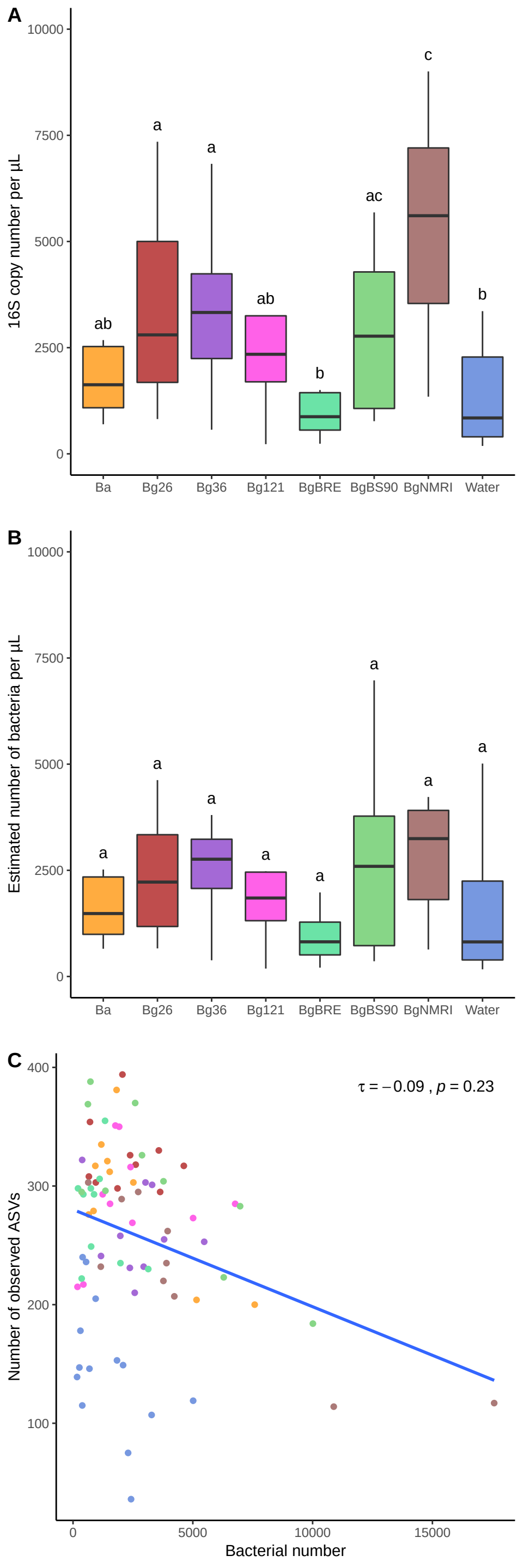
A
16S copy number per µL
10000
7500
5000
2500
0
ab
a
a
ab
b
ac
c
b
Ba
Bg26
Bg36
Bg121
BgBRE
BgBS90
BgNMRI
Water
B
Estimated number of bacteria per µL
10000
7500
5000
2500
0
a
a
a
a
a
a
a
a
Ba
Bg26
Bg36
Bg121
BgBRE
BgBS90
BgNMRI
Water
C
Number of observed ASVs
400
300
200
100
τ = −0.09 , p = 0.23
0
5000
10000
15000
Bacterial number